OPTIMIZATION OF THE 1050 NM PUMP POWER AND FIBER LENGTH IN SINGLE-PASS AND DOUBLE-PASS THULIUM DOPED FIBER AMPLIFIERS

S. D. Emami and S. W. Harun [†]

Photonics Research Center
University of Malaya
Kuala Lumpur 50603, Malaysia

F. Abd-Rahman

Faculty of Engineering and Science
Universiti Tunku Abdul Rahman
Setapak 53300, Malaysia

H. A. Abdul-Rashid and S. A. Daud

Faculty of Engineering
Multimedia University
Cyberjaya 63100, Malaysia

H. Ahmad

Photonics Research Center
University of Malaya
Kuala Lumpur 50603, Malaysia

Abstract—The pump power and thulium-doped fiber (TDF) length for both single-pass and double-pass Thulium-Doped Fiber Amplifiers (TDFA) are theoretically optimized by solving differential equations. The 1050 nm pump is used to provide both ground-state and excitedstate absorptions for amplification in the S-band region. The TDFA is saturated at a shorter length with a higher gain value as the operating pump power increases. The double-pass TDFA allows double propagation of the test signal in the gain medium, which increases the effective TDF length and thus improves the gain of the TDFA

Corresponding author: S. W. Harun (swharun@um.edu.my).
[†] S. D. Emami and S. W. Harun are also with Department of Electrical Engineering, University of Malaya, Kuala Lumpur 50603, Malaysia.

compared to the single-pass configuration. Therefore, a small signal gain improvement of approximately 15 dB is obtained in the 1465 nm region. However, a noise figure penalty of approximately 1 dB is also obtained in this wavelength region. The theoretical result is in agreement with the experimental result.

1. INTRODUCTION

Due to the tremendous increase in communication traffic in recent years, more and more efforts in research have been directed towards developing highly efficient broad-band fiber amplifiers that will fully exploit the low-loss band of silica fibers at the 1450–1630 nm range, which has a loss of only 0.25 dB/km in order to increase the transmission capacity of wavelength-division multiplexing (WDM) networks [1, 2]. These broad-band amplifiers must be able to amplify the new short wavelength band (S-band) in addition to the existing C- and L-bands. Thulium-doped fiber amplifiers (TDFAs) are a promising candidate for the S-band amplification because the amplification bandwidth of the TDFA is centered at 1470 nm [3], which falls within the S-band. A 1050 nm pumping scheme can be used to obtain the population inversion in a Thulium-doped fiber (TDF). The TDF length and pump power are the important parameters that determine the attainable gain and noise figure in TDFA.

In this paper, the pump power and TDF length for both single-pass and double-pass TDFA are theoretically optimized by solving differential equations. The TDF is pumped by a 1050 nm laser diode for both configurations. Differential equations involved in the theoretical analysis are solved using the Runge-Kutta method [4–6].

2. CONFIGURATION OF THE TDFA

The basic architecture of the single pass and double pass TDFAs are depicted in Fig. 1. Fig. 1(a) shows the setup of the single pass TDFA, which consists of a TDF, a wavelength division multiplexing (WDM) coupler, a pump laser and two isolators. The TDF used is a fluoride based one with thulium ion concentration of 2000 ppm. A WDM coupler is used to combine the pump light with the input signal. The 1050 nm laser diode is used as the pump source. Optical isolators are used to ensure unidirectional operation of the optical amplifier. In the double pass configuration of Fig. 1(b), an optical circulator is placed at the input part of the amplifier to inject an input signal and to route an amplified signal into the output port. A fiber mirror is
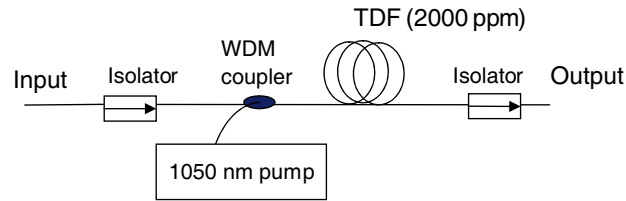
(a) single pass
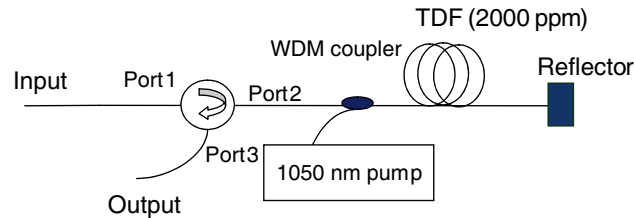
(b) double pass

Figure 1. Configuration of the TDFA. (a) Single pass, (b) double pass.

used as a reflector to reflect a selected wavelength. For simplicity, the reflected forward amplified spontaneous emission (ASE) is neglected in this work.

3. MODELING OF THE TDFA

In this work, atomic rate equations are used to describe the TDFA. In the other words, the rate equations describe the interaction between pump, signal and ASE light in the TDFA. The equations are used to estimate populations in the energy levels under any pump and signal power conditions. From the rate equations, the gain coefficient for signal light and absorption coefficient for pump light are defined by considering the absorption and stimulated emission cross sections [6]. To obtain the rate equations, an analysis of a six level energy system is discussed. Fig. 2 shows the energy level diagram of trivalent thulium ion in fluoride glass. Figs. 2(a) and (b) show the absorption and emission transitions, respectively in the TDFA with 1050 nm pump [6].

The main transition used for S-band amplification is from the $^3H_4$ to $^3F_4$ energy levels. This amplification is made possible by a multi-step pumping via excited state absorption (ESA) [4], which forms a
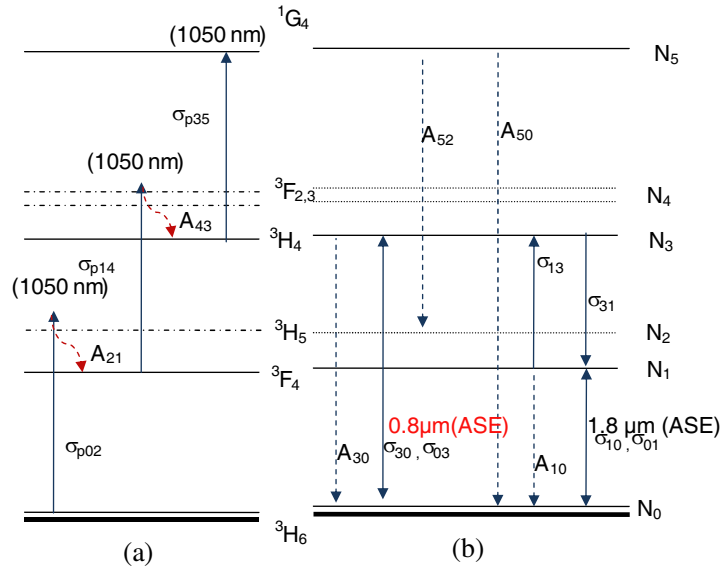
Figure 2. Pumping mechanism of a 1050 nm pumped TDFA. (a) Pump absorption, (b) signal and ASE emission transitions.

population inversion between $^3H_4$ and $^3F_4$ levels. When the TDF is pumped with 1050 nm laser, the ground state ions in the $^3H_6$ energy level can be excited to the $^3H_5$ energy level and then relaxed to the $^3F_4$ energy level by non-radiative decay. The $^3F_4$ energy level ions are then re-excited to the $^3F_2$ energy level and experience non-radiative decay to the $^3H_4$ energy level via excited state absorption [7]. The 1050 nm pump alone can provide both the ground-state and excited-state absorptions [6].

In the rate equation models, the energy level of the $^3F_2$ and $^3F_3$ energy levels are nearly the same and can be treated as one level for simplicity. The variables N_0, N_1, N_2, N_3, N_4, and N_5 are used to represent population of ions in the $^3H_6, ^3F_4, ^3H_5, ^3H_4, ^3F_2$, and $^1G_2$ energy levels respectively. According to the above figure we can write the rate of population for each layer for single pass and double TDFA

as follows [5]:

$$\frac{dN_0}{dt} = -(W_{p02} + W_{18a} + W_{8a})N_0 + (A_{10} + W_{18e})N_1$$
$$+(A_{30} + W_{8e})N_3 + A_{50}N_5 \tag{1}$$

$$\frac{dN_1}{dt} = (W_{18a})N_0 - (A_{10} + W_{p14} + W_{sa} + W_{18e})N_1$$
$$+(A_{20})N_2 + W_{se}N_3 \tag{2}$$

$$\frac{dN_2}{dt} = (W_{p02})N_0 - (A_{21}^{nr})N_2 + (W_{52})N_5 \tag{3}$$

$$\frac{dN_3}{dt} = (W_{8a})N_0 + (W_{sa})N_1 - (A_{30} + W_{p35} + W_{se} + W_{8a})N_3$$
$$+(A_{43})N_4 \tag{4}$$

$$\frac{dN_4}{dt} = (W_{p14})N_1 - (A_{43}^{nr})N_4 \tag{5}$$

$$\frac{dN_5}{dt} = (W_{p35})N_3 - (A_{50} + A_{52})N_5 \tag{6}$$

$$\sum_i N_i = \rho \tag{7}$$

where $W_{p02}, W_{p14}, W_{p35}$ are transition rates of the 1050 nm pump. Signal stimulated absorption and emission are described by W_{sa} and W_{se} respectively. The transition rates of amplified spontaneous emission (ASE) at 800 nm ($^3H_4 \rightarrow {}^3H_6$) and 1800 nm ($^3F_4 \rightarrow {}^3H_6$) are governed by W_{8e}, W_{18e} respectively. The transition rates of stimulated absorption at 800 nm ($^3H_4 \rightarrow {}^3H_6$) and 1800 nm ($^3F_4 \rightarrow {}^3H_6$) are governed by W_{8a}, W_{18a} respectively. The nonradiative transition rate from $^3F_2$ to $^3F_4$ and from $^3H_5$ to $^3F_4$ energy levels are defined as A_{43}^{nr} and A_{21}^{nr}, respectively, and A_{ij} is the radiative rate from level i to level j. Others radiative transitions are not included in the rate equations because they have an ignorable effect on the S-band amplification.

Equations (1) $\sim$ (6) can be solved by considering the steady state regime where the populations are time independent, $dN_i/dt = 0 (i = 0, 1, \ldots, 5)$. The average thulium ion concentration in the core is denoted as ρ and is quantified by [8]

$$\rho = \frac{2}{b^2} \int_0^\infty n(r) r \, dr \tag{8}$$

where b is the doping radius and $N(r)$ is the thulium ions concentration profile. The interaction of the electromagnetic field with the ions or

the transition rate (W_{ij}) for a single pass TDFA can be written as:

$$W_{p02,p14,p35} = \lambda_{P1}\sigma_{p02,p14,p35}\left(\frac{P_{P1}^{+}}{hcA_{eff}}\right) \tag{9}$$

$$W_{8a,8e,18a,18e} = \lambda_{ASE}^{8,18}\sigma_{03,30,01,10}\left(\frac{P_{ASE}^{8,18+} + P_{ASE}^{8,18-}}{hcA_{eff}}\right) \tag{10}$$

$$W_{sa,se} = \lambda_{ASE}^{8,18}\lambda_{s}\sigma_{sa,se}\left(\frac{P_{ASE}^{8,18+}+P_{ASE}^{8,18-}}{hcA_{eff}}\right)+\lambda_{s}\sigma_{sa,se}\left(\frac{P_{s}}{hcA_{eff}}\right) \tag{11}$$

where $\sigma_{p02}, \sigma_{p14}, \sigma_{p35}$ are the ${}^3\text{H}_6 \rightarrow {}^3\text{H}_5$, ${}^3\text{F}_4 \rightarrow {}^3\text{F}_2$, ${}^3\text{H}_4 \rightarrow {}^1\text{G}_4$ absorption cross sections of the 1050 nm forward pumping respectively. The stimulated absorption cross section at 800 nm is denoted by σ_{03} and the stimulated emission cross section at 800 nm and 1800 nm are denoted by σ_{30}, and σ_{10} respectively. P_p and P_s are the 1050 nm pump power and signal power respectively. σ_{sa} and σ_{se} are the stimulated absorption and the stimulated emission crosssection of input signal respectively. P_{ase}, P_{ase8}, and P_{ase18} are the amplified spontaneous emission (ASE) at S-band, 800 nm and 1800 nm, respectively in the forward $(+)$ and backward $(-)$ directions along the fiber. A_{eff} is an effective area of the TDF. The light-wave propagation equations along the thulium fiber (in the z direction) can be established as follows [7];

$$\frac{dP_{ASE}^{\pm}}{dz} = \pm\Gamma(\lambda_{ASE})(\sigma_{se}N_3 - \sigma_{se}N_1 + \sigma_{01}N_0) \times P_{ASE}^{\pm}$$
$$\pm\Gamma(\lambda_{ASE})2hv\Delta v\sigma_{se}N_3 \mp \alpha P_{ASE}^{\pm} \tag{12}$$

$$\frac{dP_{ASE}^{8\pm}}{dz} = \pm\Gamma(\lambda_8)(\sigma_{30}N_3 - \sigma_{03}N_1) \times P_{ASE}^{8\pm}$$
$$\pm\Gamma(\lambda_8)2hv\Delta v\sigma_{30}N_3 \mp \alpha P_{ASE}^{8\pm} \tag{13}$$

$$\frac{dP_{ASE}^{18\pm}}{dz} = \pm\Gamma(\lambda_{18})(\sigma_{10}N_1 - \sigma_{01}N_0) \times P_{ASE}^{18\pm}$$
$$\pm\Gamma(\lambda_{18})2hv\Delta v\sigma_{10}N_1 \mp \alpha P_{ASE}^{18\pm} \tag{14}$$

$$\frac{dP_{P1}^{+}}{dz} = -\Gamma(\lambda_{P1})(\sigma_{p02}N_0 + \sigma_{p14}N_1 + \sigma_{p02}N_3) \times P_{P1}^{+} - \alpha P_{P1}^{-} \tag{15}$$

$$\frac{dP_s}{dz} = -\Gamma(\lambda_s)(\sigma_{se}N_3 - \sigma_{sa}N_1 - \sigma_{01}N_0) \times P_s - \alpha P_s \tag{16}$$

where α is the background scattering loss, which is assumed to be constant for all wavelengths. λ_{ASE}, λ_{ASE8} and λ_{ASE18} are the signal wavelengths, 800 nm ASE and 1800 nm ASE respectively. The

overlapping factors between each radiation and the fiber fundamental mode, $\Gamma(\lambda)$ can be expressed as [8, 9]:

$$\Gamma(\lambda) = 1 - e^{-\frac{2b^2}{w_o^2}} \tag{17}$$

$$w_0 = a\left(0.761 + \frac{1.237}{V^{1.5}} + \frac{1.429}{V^6}\right) \tag{18}$$

where w_0 is the mode field radius defined by Equation (18), a is the core diameter, b is the thulium ion-dopant radius and V is the normalized frequency.

In the double pass configuration of Fig. 1(b), two signals propagate in the opposite direction of each other in the active medium. After the first signal passes through the active material, the amplifier's forward propagating signal (P_s^+) is reflected back by the fiber mirror and passes through the active material as a backward propagating signal (P_s^-) for further amplification [10]. Therefore, in order to calculate the stimulated absorption and emission rate of the double pass TDFA, both P_s^+ and P_s^- are calculated in the Equation (11) in the following way

$$W_{sa,se} = \lambda_{ASE}^{8,18}\lambda_s\sigma_{sa,se}\left(\frac{P_{ASE}^{8,18+} + P_{ASE}^{8,18-}}{hcA_{eff}}\right) + \lambda_s\sigma_{sa,se}\left(\frac{P_s^+ + P_s^-}{hcA_{eff}}\right) \tag{19}$$

The steady state populations from Level 1 to Level 6 are calculated based on the newly calculated $W_{sa,se}$ rate. The equations describing the spatial development of P_s^+ and P_s^- are written as:

$$\frac{dP_s^+}{dz} = -\Gamma(\lambda_s)(\sigma_{se}N_3 - \sigma_{sa}N_1 - \sigma_{p01}N_0) \times P_s^+ - \alpha P_s^+ \tag{20}$$

$$\frac{dP_s^-}{dz} = +\Gamma(\lambda_s)(\sigma_{se}N_3 - \sigma_{sa}N_1 - \sigma_{p01}N_0) \times P_s^- + \alpha P_s^- \tag{21}$$

The equations describing the spatial development of P_p, P_{ase}, P_{ase8}, and P_{ase18} in the double pass TDFA remain the same as that of the single pass TDFA. During the reflection of the signal by the fiber mirror, mirror losses need to be considered. The initial value of backward signal power at the end of double pass TDFA is calculated by [8]:

$$P_{\text{Sinitial}}^- = P_{\text{Sinitial}}^+ * G_{\text{firstpass}} * \text{Mirror loss} \tag{22}$$

where $G_{\text{firstpass}}$ is the gain of the signal after the first pass through the double pass TDFA and P_{Sinitial}^+ is the initial signal power in forward direction which is input into the double pass TDFA.

Noise figure is generated by spontaneous emission and therefore is closely related to ASE. The number of spontaneous photon is given by:

$$\eta = \frac{\frac{\sigma_{SE}}{\sigma_{SA}} N_3}{\frac{\sigma_{SE}}{\sigma_{SA}} N_3 - N_2} \tag{23}$$

The noise figure (NF) of the double pass TDFA at the signal wavelength is calculated as [10, 11]:

$$NF(\lambda_s) = \frac{1 + 2\eta[G - 1]}{G} \tag{24}$$

where G is the total gain of the double pass TDFA. The noise figure can also be calculated using the following equation;

$$NF = 1/G + P_{ASE}/(G \times h \times v \times \Delta v) \tag{25}$$

where P_{ASE} is the ASE power, h is Planck's constant, v is the frequency of the signal and Δv is the resolution of the measuring device such as an optical spectrum analyzer.

4. NUMERICAL CALCULATIONS

In order to solve the population rate in steady state condition, the time derivatives of Equations (1)–(6) are set to zero. All the equations used for pump and signal powers, Equations (12)–(17), are first order differential equations and the Runge-Kutta method is used to solve

Table 1. Initial condition.

Initial condition	Operating Wavelength	Explanation
$P_{P1}(z = 0) = P_{P1}$	$\lambda = 1050$	Initial condition for 1050 nm pump at $Z = 0$
$P_S(z = 0) = P_S$	-	Initial condition for signal pump at $Z = 0$
$P_{ASE}^+(z = 0, v)$ $= P_{ASE}^-(z = l, v) = 0$	$1460 < \lambda < 1050$	Initial condition for PASE $\pm$ at s-band for $Z = 0$ and $Z = L$
$P_{ASE}^{8+}(z = 0, v)$ $= P_{ASE}^{8-}(z = l, v) = 0$	$1460 < \lambda < 1050$	Initial condition for PASE $\pm$ at 800 nm for $Z = 0$ and $Z = L$
$P_{ASE}^{18+}(z = 0, v)$ $= P_{ASE}^{18-}(z = l, v) = 0$	$1460 < \lambda < 1050$	Initial condition for PASE $\pm$ at 1800 nm for $Z = 0$ and $Z = L$

these equations. In the numerical modeling, we initially assume all the population to be at the ground level ($^3H_6$). Table 1 shows the initial conditions, which are set on pump power, signal power and ASE spectrum at S-band, 800 nm and 1800 nm wavelength [11].

The thulium doped fiber with length L is divided into L segments along the z direction, as shown in Fig. 3. We solve for the pump, signal and ASE power propagating in the first segment (Segment 0) by using the above initial conditions. For the following segments (Segment 1– L-1), the power for all the pump, signal and ASE at one end of a segment is used as the input for the next segment. Relaxation method is used to achieve an accuracy of 0.01% for all the pump, signal and ASE powers [11].

The spectral emission cross-section at S-band of Thulium ion [12] and the spectral absorption cross-section at S-band can be estimated by the modified McCumber's relation [8]:

$$\sigma_{sa}(v) = \frac{\sigma_{se}(v)}{\eta^{peak}} \exp\left\{\frac{h(v - v^{peak})}{k_B T}\right\} \tag{26}$$

$$\eta^{peak} = \frac{\sigma_{se}^{peak}}{\sigma_{sa}^{peak}} \tag{27}$$

where k_B is Boltzmann constant and T is temperature. As observed experimentally, the absorption cross section peak is approximately 70% of the emission peak. Fig. 4 shows the spectra of the emission and absorption cross section of the TDF in fluoride glass, which were obtained from Equation (26).

The theoretical results are obtained by solving the rate equations of the pump, signal power and ASE using a numerical method. The variables used in the numerical calculation and their corresponding values are shown in Table 2, which is obtained from various publications [4, 12–14].
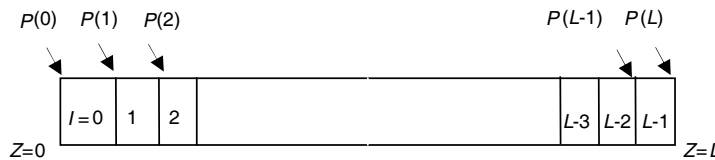
Figure 3. Schematic of the fiber model.
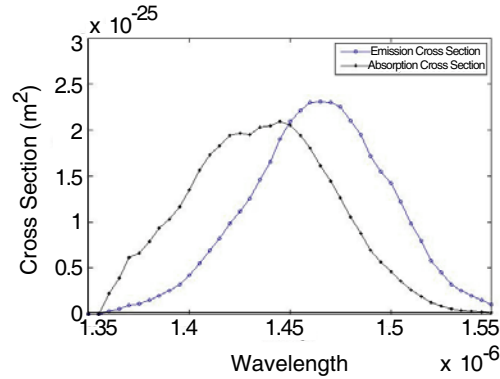
Figure 4. Emission and absorption cross section of the fluoride-based TDFA.

## 5. RESULTS AND DISCUSSION

Optimization of the length of the thulium-doped fiber (TDF) used is one of the most important issues that need to be considered for designing a TDFA in order to obtain the best gain with the lowest noise figure. In the case of remote pumping, the location of the amplifiers are far away from the source and an optimized pump power is essential. The gain and noise figure of the TDFA are strongly dependent on the TDF length and the operating pump power. The optimum TDF length is also dependent on the operating pump power and therefore a reference TDF length is firstly determined in this work. Then the operating pump power is optimised with respect to the reference TDF length. Careful considerations are necessary during the selection of the reference TDF length. If the reference TDF length is too short, the TDFA will be saturated at a very low pump power and this does not provide a high gain. Saturation takes place in TDFA due to the fixed thulium ion concentration and therefore after a certain amount of pump power, the N_3 state population climbs to an almost constant level. In our simulation, saturation is defined as the condition where the increment of gain is less than $0.4\,\text{dB}$ with respect to an increment of $1\,\text{mW}$ pump power. In the case of a short TDF, the total population is very low and hence the TDF is fully inverted by a very low amount of pump power. If this low amount of pump power is selected as the operating pump power then the optimized TDF length with respect to this low amount of pump power is very short.

Figures 5(a), (b) and (c) show the gain and noise figure of $1460\,\text{nm}$ signal as a function of pump power for both single-pass and double-

Table 2. Numerical parameter used in the simulation [4, 12–14].

Parameter	Unit	Sym	Value
Thulium concentration	$1/\text{m}^3$	ρ	1.68×10^{25}
Numerical aperture		NA	0.3
Fiber Length	m	L	20
Background lost	dB/m	α	1.68×10^{25}
Effective area	m^2	A_{eff}	2.096×10^{-12}
Division along fiber			12
800 nm ASE bandwidth	nm	Δv_8	10
1800 nm ASE bandwidth	nm	Δv_{18}	100
ASE bandwidth	nm	Δv	2
1050 nm Pump absorption cross section	m^2	σ_{p02}	1.1×10^{-27}
1050 nm Pump absorption cross section	m^2	σ_{p14}	8.2×10^{-25}
1050 nm Pump absorption cross section	m^2	σ_{p35}	2.5×10^{-27}
1650 nm Pump absorption cross section	m^2	σ_{p01}	2×10^{-26}
Signal absorption cross section	m^2	σ_{sa}	Fig. 4
Signal stimulated emission cross section	m^2	σ_{se}	Fig. 4
800 nm transition cross section	m^2	$\sigma_{03},$	6.2×10^{-25}
1800 nm transition cross section	m^2	$\sigma_{01},$	5.2×10^{-25}
Radiative decay rate	1/s	A_{10}	172.4
Radiative decay rate	1/s	A_{30}	702.8
Radiative decay rate	1/s	A_{50}	676.3
Radiative decay rate	1/s	A_{52}	492.9
Nonadiative decay rate	1/s	A_{43}^{nr}	52976
Nonadiative decay rate	1/s	A_{21}^{nr}	165626

pass TDFAs at different reference length of 12 m, 20 m and 34 m, respectively. In this simulation, the input signal power is fixed at -37 dBm. As shown in these figures, the gain for both single-pass and double-pass amplifiers increases with the increment of pump power and the gain for the double-pass amplifier is higher than that of the single-pass amplifier. On the other hand, the noise figure improves or reduces with the increment of pump power. The result clearly shows that the increment of gain and the decrement of NF are very low with respect to the increment of pump power after the pump power exceeds 100 mW for the single pass and 125 mW for the double pass TDFA. At a pump power of 100 mW and 12 m TDF length, the TDFA is able to provide a gain of 11 dB and 16 dB for thesingle-pass and double-pass configuration respectively, as shown in Fig. 5(a). If a 12 m long TDF is

(a) reference length = 12m

(b) reference length = 20m

(c) reference length = 34m
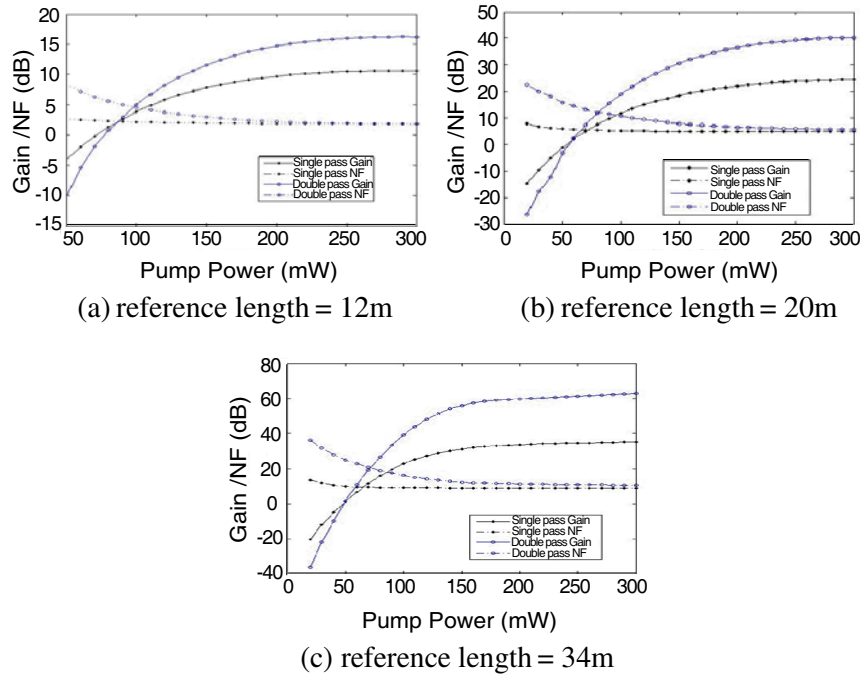
Figure 5. The gain and noise figure against pump power for both single-pass and double-pass TDFA at various reference TDF length. (a) 12 m, (b) 20 m, and (c) 34 m.

selected as a reference then based on the saturation characteristics of the TDFA as shown in Fig. 5(a), a 100 mW and 125 mW pump power should be selected as the operating pump power for single-pass and double pass TDFA configurations respectively. Since, the optimized TDF length with respect to 100 mW and 125 mW pump power is very short, the total cumulative gain of the TDFA is also very low.

On the other hand, if the length of TDF is longer then a greater pump power is required to invert the population of the entire TDF, especially toward the end of the TDF. The saturation pump power is also higher as shown in Figs. 5(b) and (c) for the reference length of 20 m and 34 m, respectively. As seen in Fig. 5(b), a gain saturation of 15 dB and 30 dB are obtained at a pump power of 120 mW and 150 mW for single-pass and double-pass TDFA respectively. Fig. 5(b) shows that the increment of gain and decrement of noise figure with respect to the increment of pump power are very low after the pump power exceeds these saturation levels. Fig. 5(c) shows that the gain saturation

of 24 and 55 dB are obtained at pump power of 130 mW and 170 mW respectively for single-pass and double-pass TDFA respectively. In the optical network, an amplifier is mainly designed to obtain a gain as high as possible with a low noise figure using a minimum pump power. Although the 34 m long TDFA architecture which has the optimum operating pump power of 170 mW is able to provide the highest gain but the use of a high pump power is in conflict with the main objective of the TDFA design which requires a smaller pump power especially for long haul applications. For this reason, a very long TDF is not recommended to be considered as a referenceTDF length during the design of single and double pass TDFAs.

The length of the TDF is also optimized by calculating the gain as a function of TDFlength for various operating pump powers as shown in Fig. 6. The input signal power and wavelength is fixed at -37 dBm and 1470 nm, respectively and the 1050 nm pump power is varied from 100 to 200 mW. The single-pass configuration of Fig. 1(a) is used in this simulation. As shown in Fig. 6, the maximum gain is obtained at 25, 31 and 34 dB with the pump powers of 100, 150 and 200 mW respectively. The maximum gain is obtained at a TDF length of 54, 41 and 36 m for pump power of 100, 150 and 200 mW, respectively. These results show that the TDFA is saturated at a shorter length with a higher gain value as the operating pump power increases. The gain gradually drops after the peak value as the TDF length increases. This is attributed to the pump power being fully absorbed in this region and saturates the gain. The upconversion, absorption and background loss inside the TDF contribute to the gain drop at the saturation region.

The ASE has a negligible effect on the total gain of both the single pass and double pass TDFAs. Fig. 7 shows a forward and backward traveling ASE power of both single-pass and double-pass TDFAs as a function of position in the TDF for different TDF length settings.
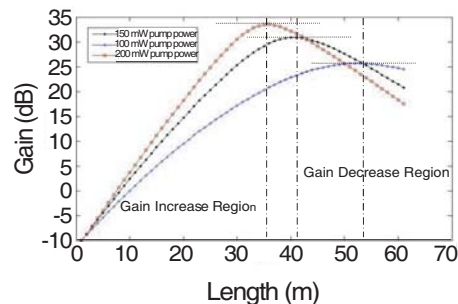
**Figure 6.** Gain against TDF length for different pump powers.
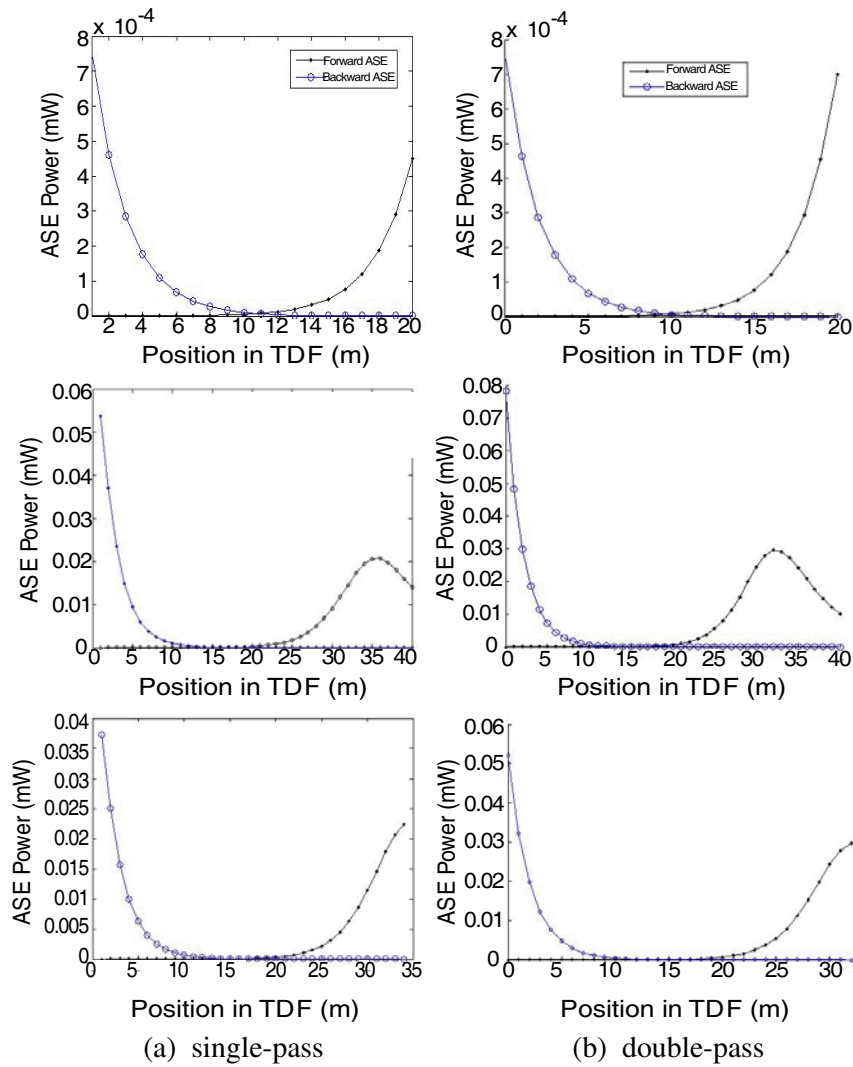
Figure 7. The forward and backward traveling ASE power against the position in TDF for both (a) single-pass and (b) double-pass TDFA.

The 1050 nm pump power is fixed at 200 mW. As shown in the figure, the backward ASE is higher than the forward ASE for both single-pass and double-pass TDFAs. For instance, the forward and backward ASE power are obtained at 0.03 mW and 0.05 mW respectively for double-pass TDFA. This is due to the inversion at the beginning of

the TDF length being much higher than the inversion at the end of TDF. The backward ASE is amplified along a well inverted piece of TDF before exiting the TDF, while the forward ASE travel along a piece of TDF that is progressively less inverted and thus has less gain per unit length than the backward ASE does. The results also show that the forward and backward ASE in the double pass configuration is higher than single pass TDFA. This is due to the higher inversion in the double-pass system, which has the backward signal.

Figure 7 also shows that the 40 m long TDF provides the highest backward ASE compared to the shorter lengths. In this TDFA, the backward ASE travels over a longer distance and become much higher at the beginning of the TDF. However, at a TDF length of more than


(a)

(b)

(c)
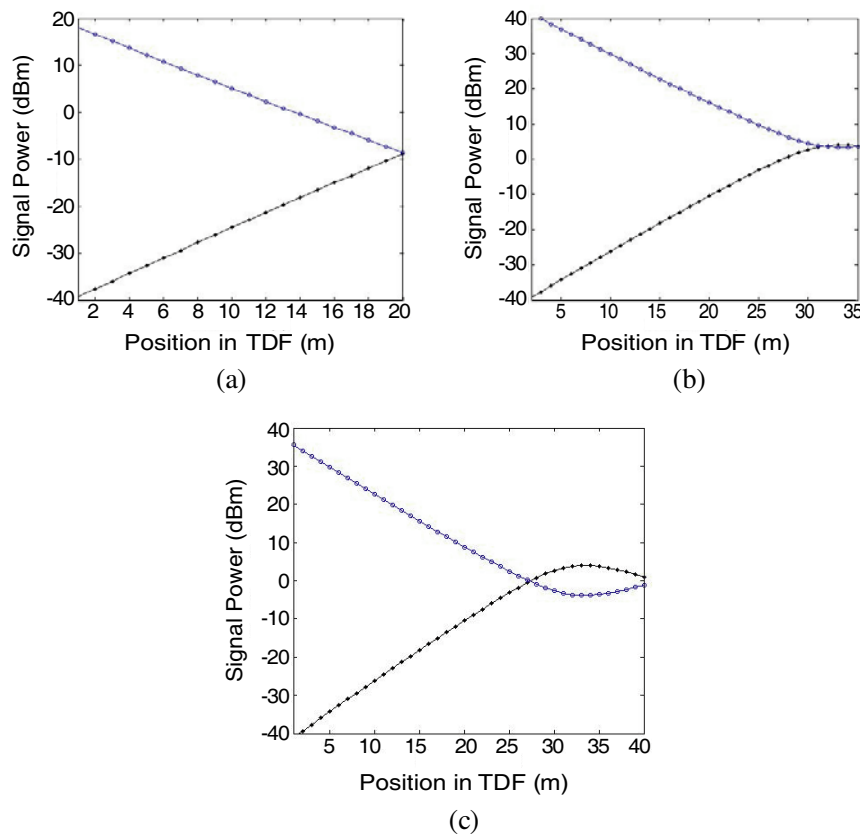
Figure 8. The propagation of the forward and backward amplified signal in the double-pass TDFA for different TDF length. (a) 20 m, (b) 35 m, and (c) 40 m.

the optimum length, the higher backward ASE depletes the inversion and robs the gain at the expense of the signal as well as forward ASE. Both signal and forward ASE powers will be reduced due to the less inverted portion of the TDF at the end.

Figure 8 shows the propagation of forward and backward amplified signals in the double-pass amplifier as a function of position along a 20, 35 and 40 m long TDF at 1470 nm signal wavelength using 200 mW pump power and an injected signal power of −40 dBm. As shown in the figure, the input forward signal is amplified to −10, 3 and −1 dBm during the first pass for 20, 35 and 40 m long TDFs of the double-pass amplifier. The signal is further amplified in the backward direction to 18, 41 and 38 dBm for the cases of 20, 35 and 40 m respectively. According to these results a 35 m long double pass TDFA provides a gain that is 3 dB higher than the 40 m long double pass TDFA. If a TDFA of length less than the optimum length is used, the backward ASE is lower at the beginning of the TDF. Thus, the depletion of the pump power is lower at the beginning of the TDF compared to at the optimum length. As a result, a portion of the pump power remains unused which causes more population inversion and hence the increment of the gain. According to these results, a 20 m long TDF provides less backward ASE than a 35 m long TDF and therefore the 35 m long double pass TDFA provides a 20 dB higher gain than the 20 m long double pass TDFA. From the above discussion the 35 m long double pass TDFA provide the maximum gain.

Figure 9 shows the comparison between our results and the experimental work by Bastos-Filho et al. [14] that represents the double-pass TDFA pumped by a 1050 nm laser diode with the same setup. In the comparison, the 1050 nm pump and input signal powers
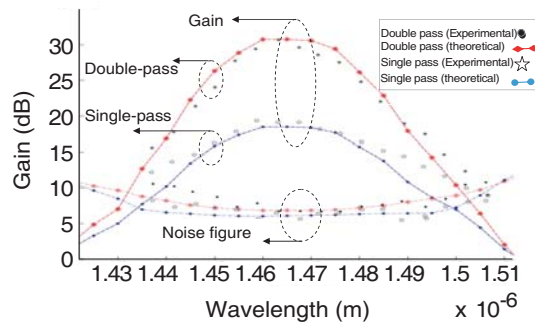
Figure 9. Gain and noise figure spectra for both single-pass and double-pass TDFAs.

are set at 250 mW and −30 dBm, respectively. The double-pass amplifier achieves a maximum gain of 32 dB at 1465 nm, which is 15 dB higher than the single-pass TDFA. The gain enhancement is attributed to the longer effective length in the double-pass TDFA. However, the noise figure is higher in the double-pass amplifier compared to the single-pass as shown in the figure. For instance, a 1 dB noise figure penalty is observed at 1470 nm in the double-pass amplifier compared with the single-pass amplifier. This increase in the noise figure is due to the counter-propagating ASE at the input part of the TDFA which reduces the population inversion at the input part of the fiber and subsequently increases the noise figure. The simulation result is in good agreement with the experimental result as shown in Fig. 9.

6. CONCLUSION

In this paper, the relation between the operating 1050 nm pump power and TDF length are studied theoretically for both single-pass and double-pass TDFA. The theoretical analysis are developed using differential equations to simulate the gain and noise figures for both TDFAs. Both amplifiers are saturated at shorter lengths with a higher gain value as the operating pump power increases. The double-pass TDFA shows a small signal gain improvement over the single-pass TDFA due to the longer effective TDF length. The improvement is approximately 15 dB in the 1465 nm region and the maximum gain is obtained at 32 dB. However, a noise figure penalty of approximately 1 dB is also observed. The theoretical result is in agreement with the experimental result.

REFERENCES

1. Caspary, R., U. B. Unrau, and W. Kowalsky, "Recent progress on S-band fiber amplifiers," *Proceedings of 5th International Conference on Transparent Optical Networks*, Vol. 1, 236–242, 2003.

2. Sakamoto, T., "S-band fiber optic amplifiers," *Conference and Exhibit on Optical Fiber Communication, OFC*, Vol. 2, TuQ1-1–TuQ1-4, 2001.

3. Kozak, M. M., R. Caspary, and W. Kowalsky, "Thulium-doped fiber amplifier for the S-band," *Proceedings of 2004 6th International Conference on Transparent Optical Networks, 2004*, Vol. 6, 51–54, 2004.

4. Yam, S. S. H. and J. Kim, "Ground state absorption in thulium-

doped fiber amplifier: experiment and modeling," *IEEE Journal of Selected Topics in Quantum Electronics*, Vol. 12, No. 4, 797–803, 2006.

5. Peterka, P., B. Faure, W. Blance, and M. Karasek, "Theoretical modeling of S-band thulium doped silica fiber amplifiers," *Optical and Quantum Electronics*, Vol. 36, 201–212, 2004.

6. Kasamatu, T., Y. Yano, and T. Ono, "1.49 μm band gain-shifted thulium doped fiber amplifier for WDM transmission system," *Journal of Lightwave Technol.*, Vol. 20, No. 10, 1826–1838, 1998.

7. Lee, W. J., B. Min, J. Park, and N. Park, "Study on the pumping wavelength dependency of S/S+-band fluoride based thulium doped fiber amplifiers," *Optical Fiber Communication Conference and Exhibit, OFC 2001*, Vol. 2, TuQ5-1–TuQ5-4, 2001.

8. Desurvire, E., *Erbium-Doped Fiber Amplifiers: Principles and Applications*, John Wiley & Sons, New York, 1994.

9. Michael, J. and F. Digonnet, *Rare-earth-doped Fiber Lasers and Amplifiers*, CRC Press, 2001.

10. Harun, S. W., N. K. Saat, and H. Ahmad, "An efficient S-band erbium-doped fiber amplifier using double-pass configuration," *IEICE Electronics Express*, Vol. 2, No. 6, 182–185, 2005.

11. Karasek, M., "Optimum design of Er3+/Yb3+ co-doped fibers for large signal high-pump-power applications," *IEEE Journal of Quantum Electronics*, Vol. 33, No. 10, 1699–1705, 1997.

12. Allen, R., L. Esterowitz, and I. Aggarwal, "An efficient 1.46 μm thulium fiber laser via a cascade process," *IEEE Journal of Quantum Electronics*, Vol. 29, No. 2, 303–306, 1993.

13. Eichhorn, M., "Numerical modeling of Tm-doped double-clad fluoride fiber amplifiers," *IEEE Journal of Quantum Electronics*, Vol. 41, No. 12, 1574–1581, 2005.

14. Bastos-Filho, C. J. A., J. F. Martins-Filho, and A. S. L. Gomes, "38 dB gain from double-pass single-pump thulium doped fiber amplifier," *IEEE Microwave and Optoelectronics Conference*, Vol. 1, 125–128, 2003.